Journal of Materials Chemistry A

COMMUNICATION

View Article Online
View Journal | View Issue

Cite this: J. Mater. Chem. A, 2016, 4, 8573

Received 15th January 2016
Accepted 9th May 2016

DOI: 10.1039/c6ta00427j

www.rsc.org/MaterialsA

Carbon nanotube containing Ag catalyst layers for efficient and selective reduction of carbon dioxide†

Sichao Ma,[ab] Raymond Luo,[c] Jake I. Gold,[c] Aaron Z. Yu,[c] Byoungsu Kim[bc] and Paul J. A. Kenis*[bc]

Over the last few decades significant progress has been made in the development of catalysts for efficient and selective electroreduction of CO_2. These improvements in catalyst performance have been of the extent that identifying electrodes of optimum structure and composition has become key to further improve throughput levels in the electrolysis of CO_2 to CO. Here we report on a simple one-step method to incorporate multi-walled carbon nanotubes (MWCNT) in the catalyst layer to form gas diffusion electrodes with different structures: (i) a "mixed" catalyst layer in which the Ag nanoparticle catalyst and MWCNTs are homogeneously distributed; and (ii) a "layered" catalyst layer comprised of a layer of MWCNTs covered with a layer of Ag catalyst. Both approaches improve performance in the electroreduction of CO_2 compared to electrodes that lack MWCNTs. The "mixed" layer performed best: an electrolyzer operated at a cell potential of −3 V using 1 M KOH as the electrolyte yielded unprecedented high levels of CO production of up to 350 mA cm^{-2} at high faradaic efficiency (>95% selective for CO) and an energy efficiency of 45% under the same condition. Electrochemical impedance spectroscopy measurements indicate that the observed differences in electrode performance can be attributed to a lower charge transfer resistance in the "mixed" catalyst layer. This study shows that a simple optimization of electrode structure and composition, *i.e.* incorporation of MWCNTs in the catalyst layer of a GDE, has a profound beneficial effect on their performance in electrocatalytic conversion of CO_2, while allowing for a lower precious metal catalyst loading with improved performance.

Current global atmospheric CO_2 levels are approximately 400 ppm and are expected to continue to rise. Already these levels impact the climate in undesirable ways as is evident from increasing sea levels, shifting climate zones, and erratic weather patterns.[1] Combined implementation of multiple approaches at a large scale such as switching to renewable energy sources, increasing the energy efficiency of buildings and vehicles, and applying underground carbon sequestration are suggested in order to significantly reduce global CO_2 emissions.[2,3] Electrochemical reduction of CO_2 to various value-added chemicals or intermediates such as carbon monoxide (CO), formate ($HCOO^-$), methane (CH_4), ethylene (C_2H_4) and alcohols is another approach that offers promise to reduce CO_2 emissions.[4–8] At the same time CO_2 electroreduction can utilize excess electrical energy from intermittent renewable sources.[4,5,9] Among the different possible products, CO is an important intermediate for the large scale production of liquid fuels through the Fischer–Tropsch process.[10]

Silver (Ag) is one of the state-of-the-art metal catalysts for electrochemically conversion of CO_2 to CO at high selectivity and current density.[4,6,11,12] Significant research efforts have been devoted to the exploration of novel Ag-based catalysts, such as organometallic Ag catalysts,[13] nanostructured Ag catalysts,[14,15] Ag particles with different particle sizes,[16] and supported Ag catalysts,[17] to improve the energy efficiency and throughput (current density) of the process. However, much fewer studies have focused on the composition and/or structure of the associated electrode, properties that are key to maximizing performance of the catalyst on the electrode. In several studies, the electrode is a metal foil,[12] or is composed of metal particles deposited on substrates such as glassy carbon electrodes in a standard three-electrode cell[16,18] or gas diffusion layers (GDL) to form a gas diffusion electrode (GDE) for an electrolyzer.[17,19–21] Use of a GDE typically improves mass transport to and from the gas–liquid-catalyst interface,[22] which is particularly important for electrochemical CO_2 conversion given the low solubility of CO_2 in water.[6] However, the electron transfer barrier between the catalyst layer and substrate, as well as the electron transfer barrier within the catalyst layer, such as deposited Ag nanoparticles (AgNPs), may limit the availability of accessible catalytic sites.

[a]Department of Chemistry, University of Illinois at Urbana-Champaign, 505 South Mathews Ave, Urbana, Illinois 61801, USA

[b]International Institute for Carbon-Neutral Energy Research (WPI-I2CNER), Kyushu University, 744 Moto-oka, Nishi-ku, Fukuoka 819-0395, Japan

[c]Department of Chemical & Biomolecular Engineering, University of Illinois at Urbana-Champaign, 600 South Mathews Ave, Urbana, Illinois 61801, USA. E-mail: kenis@illinois.edu

† Electronic supplementary information (ESI) available. See DOI: 10.1039/c6ta00427j

Since their discovery in 1991,[23] carbon nanotubes have been recognized as a class of carbon materials with interesting properties for a broad range of applications.[24] Carbon nanotubes are porous and hydrophobic, which helps to facilitate gas transport; they are mechanically stable and extremely conductive, and are reported to have electronic interaction with catalytically active species, and thus potentially suitable as support materials for electrocatalysts.[24] The rapid development of chemical vapor deposition has enabled large scale production of multi-walled carbon nanotubes (MWCNTs) at reduced cost, and thus their potential use in cost effective applications.[24,25] Several studies have already shown that the use of carbon nanotubes as the catalyst support improves metal nanoparticle catalytic performance in fuel cell applications.[24,26,27] Depending on the specific example, use of the carbon support prevents nanoparticle aggregation, provides a better conductive network, and/or enhances mass activity by lowering the noble metal loading. However, to our knowledge, how the structure of the catalyst layer that incorporates MWCNT affects electrode performance has never be studied. To date only a few research efforts have focused on use of carbon nanotubes as support materials[21] or directly as catalysts[28] in electrodes for CO_2 reduction, however, to date no study has used MWCNTs to improve the performance of metal nanoparticle catalysts.

Here, we report how the CO_2 reduction reaction can be improved by incorporating MWCNTs into the catalyst layer of a AgNP-based GDE, either in a "layered" or "mixed" fashion, compared to AgNP-based GDEs that lack MWCNTs in the catalyst layer. The reasons for the observed differences in performance are elucidated using electrochemical impedance spectroscopy (EIS). We also show that a smaller amount of precious AgNPs is needed to achieve similar performance levels when incorporating MWCNTs in the catalyst layer.

Three different electrode structures, as illustrated in Fig. 1, were investigated in this work. Electrode structure 1 (ES1) is comprised of a layer of AgNPs deposited directly on a GDL (most commonly used approach); electrode structure 2 is composed of an AgNP layer on top of a MWCNT layer deposited on a GDL (ES2 or "layered"); electrode structure 3 is comprised of a layer of a uniform mixture of AgNPs and MWCNTs deposited on a GDL (ES3 or "mixed"). The total mass of the catalyst layer (the mass of catalyst + MWCNT) was kept constant at 1 mg cm^{-2}. Therefore, the Ag loading is 1 mg cm^{-2} for ES1 and 0.5 mg cm^{-2} for ES2, while in ES3, the Ag loading varies with the Ag-to-MWCNT ratio used: for the 1 : 1 Ag/MWCNT sample, the Ag loading is 0.5 mg cm^{-2}; for the 1 : 4 Ag/MWCNT sample, the Ag loading is 0.2 mg cm^{-2}; and for the 1 : 9 Ag/MWCNT sample, the Ag loading is 0.1 mg cm^{-2}. For comparison, we also created ES1-type electrodes with respective Ag loadings of 0.1, 0.2, and 0.5 mg cm^{-2}.

Top-down views of the surface of the different GDEs obtained by scanning electron microscopy (SEM) are shown in Fig. 2. ES1 and ES2 exhibit similar morphologies as expected, since the top layer of both GDEs is composed of AgNPs. On both surfaces of ES1 and ES2, Ag nanoparticles agglomerated into bigger chunks. In contrast, agglomeration of Ag nanoparticles is not as evident on the surface of ES3. The Ag agglomerates that are visible seem to be in close contact with the MWCNTs and are distributed uniformly within the MWCNTs.

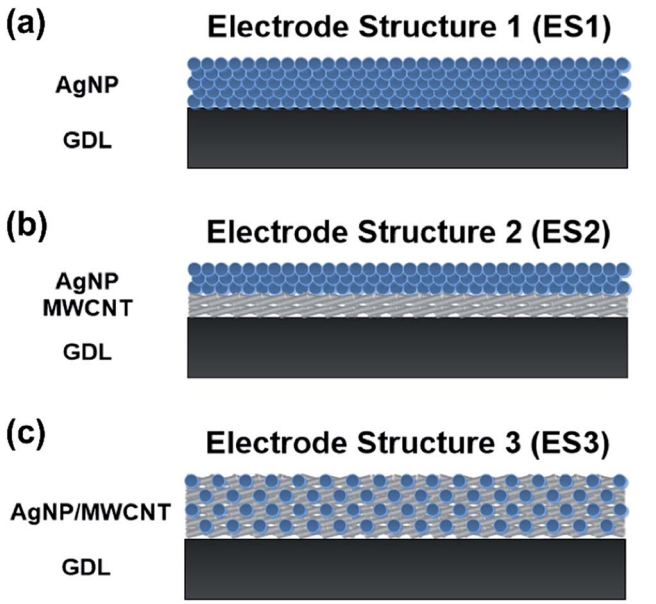

Fig. 1 Three electrode structures that were applied in this work: electrode structure 1 (ES1) is comprised of a layer of AgNPs deposited directly on a gas diffusion layer (GDL); electrode structure 2 (ES2, "layered") is composed of an AgNP layer on top of a MWCNT layer deposited on a GDL; electrode structure 3 (ES3, "mixed") is comprised of a layer of a uniform mixture of AgNPs and MWCNTs deposited on a GDL. Not drawn to scale.

The electrochemical performance of the GDEs with different electrode structures was examined using an electrochemical flow reactor that we have reported on previously.[17,19,29] In brief, an alkaline electrolyte flows between cathode and anode GDEs and refreshes the electrode surface with ions, while CO_2 gas diffuses through the GDE and reacts at the triple boundary of gas phase, electrode and electrolyte to form CO. This flow cell based on GDEs separated by a flowing electrolyte minimizes mass transfer limitations, improves throughput, and allows for tailoring of the conditions at the catalyst surface through the composition of the electrolyte. As before, the products of the electrochemical reduction of CO_2 in the gaseous effluent can be analyzed using a gas chromatography (GC) equipped with a thermal conductivity detector. The only gaseous cathode products detected were CO and H_2, which is consistent with our previous work when using Ag catalysts.[17,19] Other products such as methane may have formed as well,[12] but in quantities that are below the detection level of the TCD detector used in GC analysis of the products. The geometric area of the electrode was used to calculate current densities similar to prior related work[30,31] since measuring the electrochemical active area of Ag on GDEs is difficult. However, we did calculate the relative difference in electroactive surface area of ES1 and ES3 (Section IV in the ESI†) to show that ES3 does not have a higher electroactive surface area than ES1 due to the lower Ag loading in ES3 electrodes, even though Ag nanoparticles were less aggregated

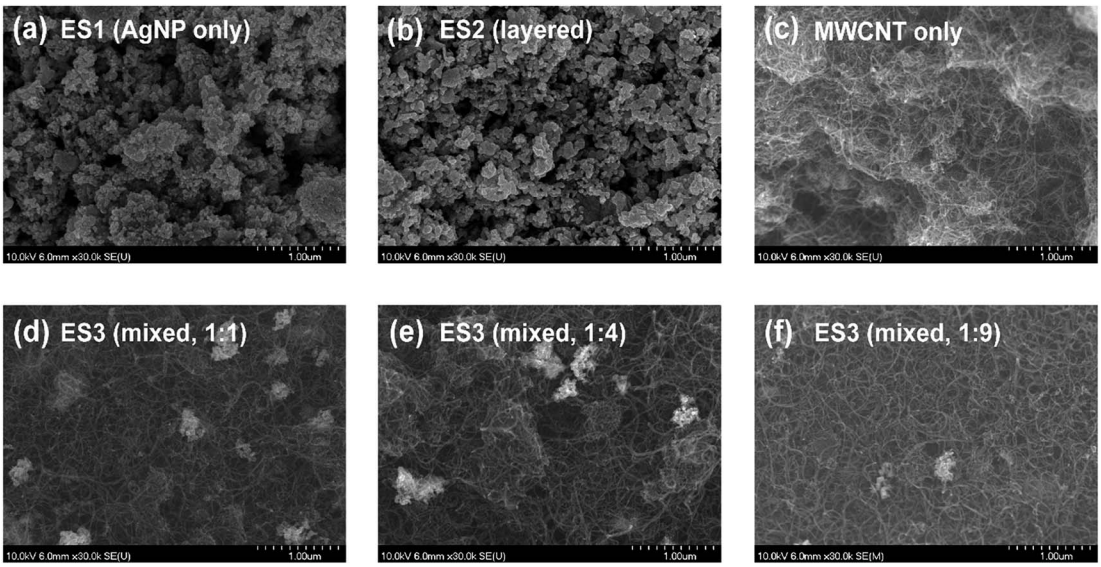

Fig. 2 SEM characterization of the surface of different electrode structures: (a) ES1 (AgNPs layer only); (b) ES2 (AgNPs layer on top of a MWCNT; "layered"); (c) control electrode with only MWCNT on the surface; (d)–(f) ES3 (catalyst layer comprised of AgNPs and MWCNT; "mixed"; in different ratios: 1 : 1, 1 : 4, and 1 : 9).

in ES3 as shown Fig. 2. Fig. 3a shows the partial current density for CO (j_{CO}) as a function of cathode potential for GDEs with different electrode structures: ES1, ES2 ("layered", Ag/MWCNT = 1 : 1), and ES3 ("mixed", Ag/MWCNT = 1 : 1). Also, to determine the activity of MWCNT for CO_2 reduction to CO in the absence of AgNPs a GDE covered with MWCNT only was tested. The GDE with ES2 achieves a higher j_{CO} than the GDE with ES1, the typical catalyst layer structure used in prior work.[17,19] The improvement in j_{CO} after adding a layer of MWCNT between the Ag layer and GDL probably can be attributed to the increased charge transfer between the Ag layer and the GDL substrate. The GDE with ES3 achieves the highest j_{CO} among all GDEs tested: a j_{CO} as high as 338 mA cm^{-2} at a cathode potential of −0.77 V *vs.* RHE. This performance level represents a more than 2-fold increase compared to the performance achieved by ES1, which exhibited the highest performance under the same condition in prior studies (*e.g.*, 164 mA cm^{-2} at a cathode potential of −0.81 V *vs.* RHE).[19] Also, ES3 exhibits a higher j_{CO} than ES2, indicating that the approach to truly integrate the MWCNT within the catalyst layer ("mixed" instead of "layered") positively affects the performance. In the "mixed" configuration (ES3), the AgNPs only exhibit minimal agglomeration and are more uniformly distributed than in ES2 as mentioned above (Fig. 2c–e *vs.* b). Furthermore, increased contact between the Ag nanoparticles and the MWCNTs in the "mixed" structure of ES3 compared to the "layered" structure in ES2, is expected to minimize charge transfer resistance within the catalyst layer. A similar trend can be observed when using carbon black (Vulcan, XC-72R) instead of MWCNT in the electrodes with ES2 and ES3 structures (Fig. S2†). The ES3 electrode with Vulcan exhibits higher j_{CO} compared to the ES2 electrode with Vulcan. Also, for the same catalyst layer structure, the electrode with MWCNT exhibits higher performance than the electrode with Vulcan, indicating that MWCNT is a more preferred carbon material than Vulcan in the catalyst layer.

The GDEs with "mixed" and "layered" structures also exhibit a significantly higher Ag utilization than the GDE with only AgNPs in the catalyst layer (ES1). The Ag loading in ES2 and the ES3 with the Ag/MWCNT ratio of 1 : 1 (0.5 mg cm^{-2}) is only half of the Ag loading in ES1 (1 mg cm^{-2}), while the j_{CO} achieved using ES2 and ES3 is about 2 times higher than when using ES1. In contrast, decreasing the Ag loading to 0.1 mg cm^{-2}, 0.2 mg cm^{-2} or 0.5 mg cm^{-2} in ES1 results in lower j_{CO} compared to the ES1 electrode with the Ag loading of 1.0 mg cm^{-2} (data shown in Fig. S3†), which further indicates that incorporating MWCNT into the catalyst layer improves accessibility of active sites of the Ag catalysts.

Fig. 3b shows the faradaic efficiencies as a function of cathode potentials for GDEs with different electrode structures. At low overpotentials, ES3 exhibits the highest faradaic efficiency (=selectivity) for CO among all GDEs, indicating that the improved charge transfer between Ag and MWCNT increases the activity for Ag to reduce CO_2 to CO. At high overpotentials, all the GDEs with AgNPs in the catalyst layer exhibit a j_{CO} on the order of 200 mA cm^{-2} (Fig. 3a) and all exhibit similar high faradaic efficiencies for CO (>90%, Fig. 3b). In contrast, the electrode covered only with MWCNTs (no Ag catalyst) exhibits a much lower j_{CO} (<100 mA cm^{-2}, Fig. 3a), and a lower faradaic efficiency for CO of only 50%. Therefore, the improvement achieved when mixing MWCNT and Ag nanoparticles is not due to the activity of MWCNT, but probably due to the enhanced charge transfer within the catalyst layer (*vide infra*), thereby increasing the Ag catalyst utilization.

We used ES3 ("mixed"), the electrode structure that exhibits the highest performance, as a model to study how the ratio of Ag to MWCNT affects the electrochemical performance. Ag-to-MWCNT ratios of 1 : 1, 1 : 4, and 1 : 9 were used, resulting in Ag

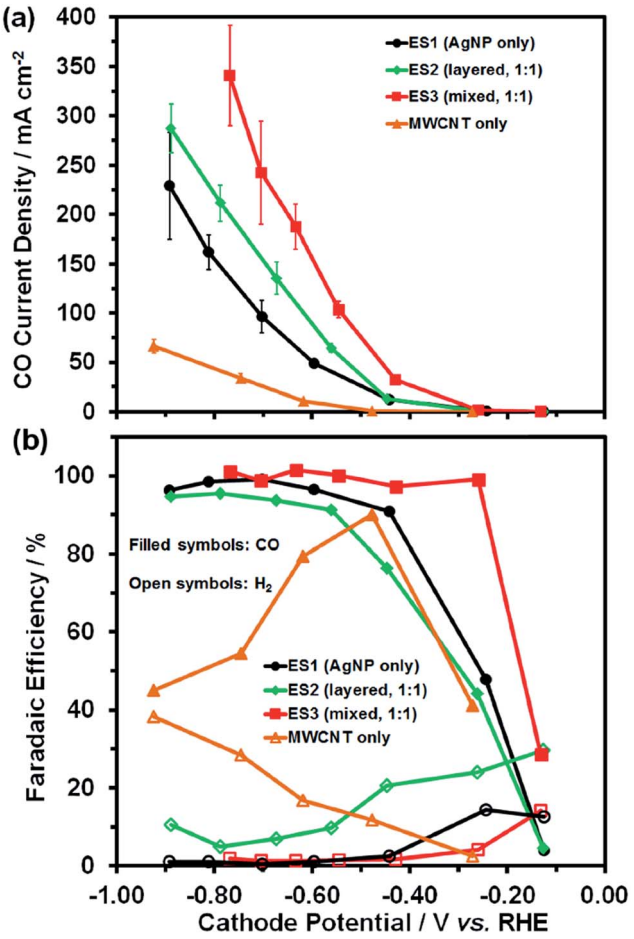

Fig. 3 (a) Partial current density for CO and (b) faradaic efficiencies for CO and H_2 as a function of cathode potential for electrodes with different structures: ES1 (AgNP only), ES2 (AgNP layer on top of a MWCNT layer; "layered"; Ag/MWCNT ratio of 1 : 1), ES3 (catalyst layer comprised of AgNPs and MWCNT; "mixed"; Ag/MWCNT ratio of 1 : 1), and a control electrode (MWCNT layer only). The total catalyst layer loading (Ag + MWCNT mass) for all electrodes is 1 mg cm^{-2}. All electrode potentials were iR-corrected.

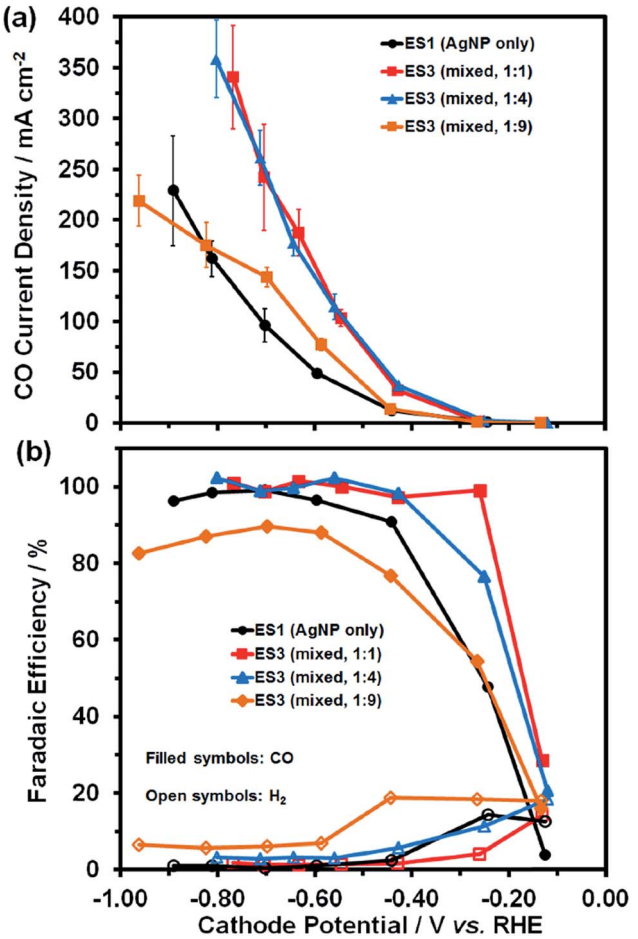

Fig. 4 (a) Partial current density for CO and (b) faradaic efficiencies for CO and H_2 as a function of cathode potential for the ES1 electrode (AgNP only) and ES3 electrodes ("mixed" catalyst layer; AgNPs and MWCNT ratios of 1 : 1, 1 : 4, and 1 : 9). The total catalyst layer loading (Ag + MWCNT mass) is 1 mg cm^{-2}. All electrode potentials were iR-corrected.

loadings of 0.5, 0.2, and 0.1 mg cm^{-2}, respectively. The results of CO_2 electrolysis using these three electrodes as well as ES1 (Ag loading of 1 mg cm^{-2}) are shown in Fig. 4. The ES3 electrodes with Ag loadings of 0.5 and 0.2 mg cm^{-2} achieve similar j_{CO} levels as high as 340 mA cm^{-2}, while the ES3 with Ag loading of 0.1 mg cm^{-2} exhibits a lower maximum j_{CO} of 200 mA cm^{-2}. At low overpotentials (more positive than -0.8 V_{RHE}), the j_{CO} for the ES3 electrode with a Ag loading of 0.1 mg cm^{-2} is higher than the j_{CO} for ES1, whereas at high overpotentials (more negative than -0.8 V_{RHE}), the ES3 electrode with a Ag loading of 0.1 mg cm^{-2} performs less well than the ES1 electrode. This observation can be attributed to the relative low faradaic efficiency for CO when using the electrode with a Ag loading of 0.1 mg cm^{-2} compared to the other electrodes (Fig. 4b). The GDE with Ag loading of 0.1 mg cm^{-2} (Fig. 4b) and the GDE with only MWCNT in the catalyst layer (Fig. 3b) showed a similar trend in the faradaic efficiencies for CO in that it drops for both electrodes at high overpotentials. In summary, when the AgNP/MWCNT ratio in the electrode is below 1 : 4, its performance becomes more similar to the GDE covered with MWCNT only (no Ag catalyst). In this study, the ES3 electrode with the AgNP/MWCNT ratio of 1 : 4 has the optimum Ag loading since it achieves the highest j_{CO} (350 mA cm^{-2}) at a Ag loading of only 0.2 mg cm^{-2}. This corresponds to a mass activity of 1750 mA cm^{-2} mg^{-1} compared to 800 mA cm^{-2} mg^{-1} for the ES1 electrode with a Ag loading of 0.2 mg cm^{-2} (Fig. S2†).

To determine how electrode structure and Ag loading within the catalyst layer affect electrode performance, we used electrochemical impedance spectroscopy (EIS) to measure the ohmic resistance (R_{cell}, which includes electrode resistance, contact resistance, electrolyte resistance, *etc.*) and charge transfer resistance (R_{ct}, the resistance determined by the heterogeneous charge transfer kinetics) of electrolysis cells composed of an IrO_2 anode and cathodes with different electrode structures and Ag/MWCNT ratios. Since all cell components and conditions except for the cathodes are the same, the difference in R_{ct} values should reflect the difference in charge transfer resistance for the cathodes studied. The experimental

data was fitted using the Boukamp model as previously reported.[32,33] In EIS the potentiostatic mode was used at a cell potential of −2.00 V. The ohmic resistance of the cell (R_{cell}, the left intercept of the hemi-circle with the *x*-axis) is almost the same for cells with different cathodes (Fig. 5). The slight differences in R_{cell} are probably due to differences in contact resistance between each assembled cell. The charge transfer resistance of the cell (R_{ct}, the right intercept of the hemi-circle with the *x*-axis) varies significantly when different cathodes were used. Specifically, the R_{ct} of the ES3 electrodes with Ag/MWCNT ratios of 1 : 1 and 1 : 4 is much smaller than the R_{ct} of the ES1 electrode, the ES2 electrode, and the ES3 electrode with a Ag/MWCNT ratio of 1 : 9. Also, the R_{ct} values of the ES2 and the ES3 electrodes are generally smaller than the R_{ct} value of the ES1 electrode. These results are in good agreement with the results shown in Fig. 3a, where the ES3 electrodes with Ag/MWCNT ratios of 1 : 1 and 1 : 4 exhibit higher j_{CO} levels than the ES1 electrode, the ES2 electrode, and the ES3 electrode with a Ag/MWCNT ratio of 1 : 9. These results show that ES3 has the highest CO_2 reduction rate, while ES1 has the lowest CO_2 reaction rate, further indicating that the approach to incorporate MWCNT into the catalyst layer affects charge transfer resistance within the catalyst layer: the electrodes with "mixed" structure and optimum Ag/MWCNT ratios (1 : 1 and 1 : 4) exhibit a higher charge transfer rate than the electrodes with a "layered" structure; therefore the former facilitates the catalytic conversion of CO_2 to CO better since the improved charge transfer from MWCNT to Ag in the MWCNT incorporated electrodes increases the charge density on the Ag catalysts, therefore leading to the improved electron transfer rate from Ag to CO_2.

The improvement in the partial current densities for CO production after incorporating MWCNT in the catalyst layers of the electrodes also leads to an increase in energy efficiency (calculated using a method described earlier[4]). Fig. 6 compares energy efficiency as a function of current density for cells using the different cathodes studied here. The ES2 electrode and the ES3 electrodes achieve higher energy efficiencies than the ES1 electrode. For the ES3 electrode with a Ag/MWCNT ratio of 1 : 4, the energy efficiency is still at 45.4% even at the highest current density of 350 mA cm^{-2}. In our prior work, we also achieved 45% energy efficiency but at a lower j_{CO} of 250 mA cm^{-2} using an ES1-type Ag electrode in 1 M KOH.[34] So the ES3 electrode studied here achieves a similar energy efficiency at a significantly higher current density. Indeed, a high overall energy efficiency in combination with high rates of CO_2 conversion will be essential for this type of electrolysis technology being transitioned to an economically viable process. Based on the same prior work that focused on optimizing electrolyte composition,[34] the ES3 electrode studied here may perform even better when using 3 M (instead of 1 M) KOH as the electrolyte.

In summary, we report a significant level of improvement in the conversion of CO_2 to CO through electrode structure modifications, specifically through incorporation of MWCNTs into the Ag catalyst layer of gas diffusion electrodes. Electrodes with uniformly mixed Ag and MWCNT as its catalyst layer exhibit higher current density (350 mA cm^{-2}), than electrodes in which the catalyst layer is comprised of a Ag layer on top of a MWCNT layer (280 mA cm^{-2}). Both types of electrodes with MWCNTs incorporated in their catalyst layer show higher performance than GDEs that lack MWCNTs (230 mA cm^{-2} at same operation conditions but at a lower Ag loading). From EIS measurements we conclude that the observed improvement in current density upon the incorporation of MWCNTs is due to a decrease in charge transfer resistance within the catalyst layer.

This work demonstrates that optimization of the electrode, here the composition and structure of the cathode catalyst layer, leads to improvement in CO_2 electrolysis performance. The high current density of 350 mA cm^{-2} observed for the "mixed" electrode ES3 (one of the highest values reported in the literature to date) holds promise for developing this electrolysis

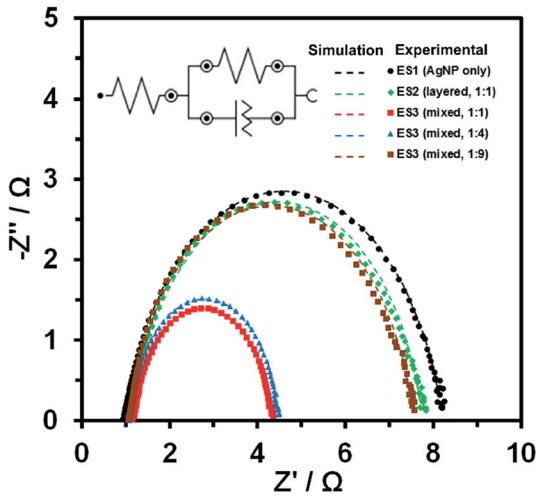

Fig. 5 Nyquist plot obtained *via* electrochemical impedance spectroscopy at a cell potential of −2.00 V for cells with different electrodes. The symbols represent experimental data while the dashed lines (under the symbols due to excellent fit) represent simulated curves using the Boukamp model.[32]

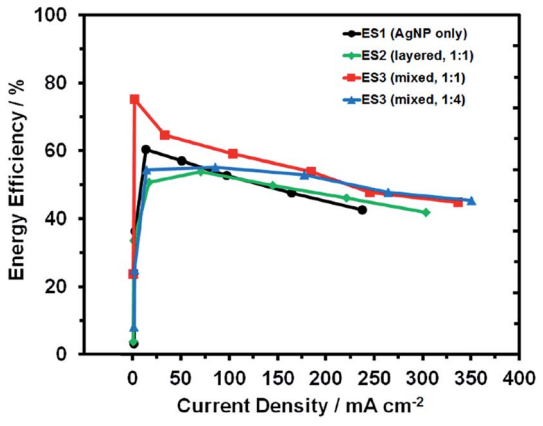

Fig. 6 Energy efficiency as a function of current density for CO_2 electrolysis cells using different electrodes: ES1 electrode (AgNP only), ES2 electrode ("layered", 1 : 1) and ES3 electrodes ("mixed"; Ag/MWCNT ratio 1 : 1 or 1 : 4). The total catalyst layer loading (Ag + MWCNT mass) is 1 mg cm^{-2}.

technology further, especially when considering the high energy efficiency of 45% at which this CO_2 conversion rate is achieved. Further optimization of electrodes with respect to the composition and structure of components other than the catalyst layer, *i.e.*, the microporous layer and the macroporous layer, may be necessary to further increase the performance, thereby bringing this technology closer to becoming an economical viable process for CO_2 mitigation and/or utilization.

Acknowledgements

We gratefully acknowledge the support of the International Institute for Carbon-Neutral Energy Research (WPI-I2CNER), sponsored by the Japanese Ministry of Education, Culture, Sports, Science and Technology. SM acknowledges support from FMC Educational Fund for a FMC Graduate Fellowship.

References

1 J. Hansen, P. Kharecha, M. Sato, V. Masson-Delmotte, F. Ackerman, D. J. Beerling, P. J. Hearty, O. Hoegh-Guldberg, S.-L. Hsu, C. Parmesan, J. Rockstrom, E. J. Rohling, J. Sachs, P. Smith, K. Steffen, L. Van Susteren, K. von Schuckmann and J. C. Zachos, *PLoS One*, 2013, **8**, e81648.
2 S. Pacala and R. Socolow, *Science*, 2004, **305**, 968–972.
3 P. Taylor, *Energy Technology Perspectives*, International Energy Agency, 2010.
4 H.-R. M. Jhong, S. Ma and P. J. A. Kenis, *Curr. Opin. Chem. Eng.*, 2013, **2**, 191–199.
5 D. T. Whipple and P. J. A. Kenis, *J. Phys. Chem. Lett.*, 2010, **1**, 3451–3458.
6 Y. Hori, in *Modern Aspects of Electrochemistry*, ed. C. Vayenas, R. White and M. Gamboa-Aldeco, Springer, New York, 2008, vol. 42, ch. 3, pp. 89–189.
7 M. Gattrell, N. Gupta and A. Co, *J. Electroanal. Chem.*, 2006, **594**, 1–19.
8 A. M. Appel, J. E. Bercaw, A. B. Bocarsly, H. Dobbek, D. L. DuBois, M. Dupuis, J. G. Ferry, E. Fujita, R. Hille, P. J. A. Kenis, C. A. Kerfeld, R. H. Morris, C. H. F. Peden, A. R. Portis, S. W. Ragsdale, T. B. Rauchfuss, J. N. H. Reek, L. C. Seefeldt, R. K. Thauer and G. L. Waldrop, *Chem. Rev.*, 2013, **113**, 6621–6658.
9 A. J. Martin, G. O. Larrazabal and J. Perez-Ramirez, *Green Chem.*, 2015, **17**, 5114–5130.
10 M. E. Dry, *Catal. Today*, 2002, **71**, 227–241.
11 Y. Hori, H. Wakebe, T. Tsukamoto and O. Koga, *Electrochim. Acta*, 1994, **39**, 1833–1839.
12 T. Hatsukade, K. P. Kuhl, E. R. Cave, D. N. Abram and T. F. Jaramillo, *Phys. Chem. Chem. Phys.*, 2014, **16**, 13814–13819.
13 C. E. Tornow, M. R. Thorson, S. Ma, A. A. Gewirth and P. J. A. Kenis, *J. Am. Chem. Soc.*, 2012, **134**, 19520–19523.
14 Q. Lu, J. Rosen, Y. Zhou, G. S. Hutchings, Y. C. Kimmel, J. G. Chen and F. Jiao, *Nat. Commun.*, 2014, **5**, 3242.
15 M. S. Jee, H. S. Jeon, C. Kim, H. Lee, J. H. Koh, J. Cho, B. K. Min and Y. J. Hwang, *Appl. Catal., B*, 2016, **180**, 372–378.
16 A. Salehi-Khojin, H.-R. M. Jhong, B. A. Rosen, W. Zhu, S. Ma, P. J. A. Kenis and R. I. Masel, *J. Phys. Chem. C*, 2012, **117**, 1627–1632.
17 S. Ma, Y. Lan, G. M. J. Perez, S. Moniri and P. J. A. Kenis, *ChemSusChem*, 2014, **7**, 866–874.
18 H. Mistry, R. Reske, Z. Zeng, Z.-J. Zhao, J. Greeley, P. Strasser and B. R. Cuenya, *J. Am. Chem. Soc.*, 2014, **136**, 16473–16476.
19 S. Ma, R. Luo, S. Moniri, Y. Lan and P. J. A. Kenis, *J. Electrochem. Soc.*, 2014, **161**, F1124–F1131.
20 H.-R. M. Jhong, F. R. Brushett and P. J. A. Kenis, *Adv. Energy Mater.*, 2013, **3**, 589–599.
21 P. Kang, S. Zhang, T. J. Meyer and M. Brookhart, *Angew. Chem., Int. Ed.*, 2014, **53**, 8709–8713.
22 R. O'Hayre, D. M. Barnett and F. B. Prinz, *J. Electrochem. Soc.*, 2005, **152**, A439–A444.
23 S. Iijima, *Nature*, 1991, **354**, 56–58.
24 M. Melchionna, S. Marchesan, M. Prato and P. Fornasiero, *Catal. Sci. Technol.*, 2015, **5**, 3859–3875.
25 J.-P. Tessonnier, M. Becker, W. Xia, F. Girgsdies, R. Blume, L. Yao, D. S. Su, M. Muhler and R. Schlögl, *ChemCatChem*, 2010, **2**, 1559–1561.
26 A. Kongkanand, S. Kuwabata, G. Girishkumar and P. Kamat, *Langmuir*, 2006, **22**, 2392–2396.
27 G. Wu and B.-Q. Xu, *J. Power Sources*, 2007, **174**, 148–158.
28 J. Wu, R. M. Yadav, M. Liu, P. P. Sharma, C. S. Tiwary, L. Ma, X. Zou, X.-D. Zhou, B. I. Yakobson, J. Lou and P. M. Ajayan, *ACS Nano*, 2015, **9**, 5364–5371.
29 D. T. Whipple, E. C. Finke and P. J. A. Kenis, *Electrochem. Solid-State Lett.*, 2010, **13**, B109–B111.
30 C. Delacourt, P. L. Ridgway, J. B. Kerr and J. Newman, *J. Electrochem. Soc.*, 2008, **155**, B42–B49.
31 J. Wu, P. P. Sharma, B. H. Harris and X.-D. Zhou, *J. Power Sources*, 2014, **258**, 189–194.
32 B. A. Boukamp, *Solid State Ionics*, 1986, **20**, 31–44.
33 L. Giorgi, A. Pozio, C. Bracchini, R. Giorgi and S. Turtù, *J. Appl. Electrochem.*, 2001, **31**, 325–334.
34 S. Verma, X. Lu, S. Ma, R. I. Masel and P. J. A. Kenis, *Phys. Chem. Chem. Phys.*, 2016, **18**, 7075–7084.

